

Re-cycling of DNA-containing Capsids Enhances Hepatitis B Virus Infection

Rupchand Sutradhar and D C Dalal

Abstract

Hepatitis B virus (HBV) infection is a deadly liver disease. A part of the newly produced HBV DNA-containing capsids are reused as a core particle in HBV replication. It is investigated that the recycling of HBV capsids greatly affects the intercellular dynamics of HBV infection. The main purpose of the present work is to study the recycling effects of HBV DNA-containing capsids in the HBV infection. Incorporating the recycling effects of capsids, a four-compartment mathematical model is proposed for the first time in order to understand the dynamics of HBV infection in a better way. The well-posedness of the model is obtained by showing non-negativity, boundedness, and uniqueness of the solution. The explicit formula for the basic reproduction number is determined by applying the next-generation approach method. The proposed model is solved with help of fourth-order explicit Runge-Kutta method. Through a rigorous comparison with experimental data obtained from four chimpanzees, the proposed model demonstrates a strong correspondence with the dynamics of HBV infection. A comprehensive global sensitivity analysis is also conducted to identify the most positively as well as negatively sensitive parameters for each compartment in the model. In the context of biology, depending on the value of basic reproduction number, the present model possesses two global asymptotically stable steady states: disease-free and endemic. The present study shows that the consideration of recycling of capsids reverses the existing mechanism of infection dynamics. This study also reveals that the accumulation of capsids within the infected hepatocytes is a key factor for exacerbating the disease. Moreover, another major finding of our study is that due to recycling of capsids, the number of released viruses increases in spite of low virus production rate. The recycling of HBV DNA-containing capsids acts as a positive feedback loop in the viral infection.

Keywords: Hepatitis B; Capsids; Recycling effects; Stability; Lyapunov functional; Numerical simulation.

Background

Hepatitis B virus (HBV) causes a deadly liver disease. As reported by the World Health Organization (WHO), around 296 million people worldwide suffer from the chronic HBV infection, where 1.5 million new cases were found each year. It was estimated that 820 000 people died due to hepatitis B virus infection in the year 2019 alone, most of them had either cirrhosis or hepatocellular carcinoma (HCC) [1]. An important factor contributing to this large number of infected humans is the disease transmission rate. Naturally, there are two types of HBV infection: acute and chronic. In the acute phase of infection, HBV DNA copies may reach as high as 10^{10} copies/ml. Acute infection typically lasts a few weeks and are eventually cured as a result of immune response [2, 3]. As for the adult population, there is a clearance rate of 85-95% in acute infection. However, chronic infections can last for many years and may result in diseases, such as liver cirrhosis and HCC [4]. Chronic infection generally is a life-long incurable condition which affects the personal impacts of the patient such as stigma and discrimination, anxiety about disease progression, and long-term health care costs etc. According to the literature and clinical findings, horizontal and vertical transmission of this virus are the two main modes of transmission to human populations. Blood transfusions, unprotected sex, reusing syringes and blades, and the reuse of medical equipment during surgery are examples of horizontal transmission. A complete understanding of the mechanisms of HBV persistence remains elusive. Consequently, HBV is a significant health concern for the population of the World.

The replication process of HBV is quite complex. In the course of infection, virion particles enter into the hepatocytes by the NA(+)-taurocholate co-transporting polypeptide (NTCP) receptor via endocytosis and uncoat themselves. The relaxed circular DNA (rcDNA) is delivered into the nucleus and is converted to covalently closed circular DNA (cccDNA) by the host DNA repair mechanism [5, 6]. RNA polymerase IIs (RNA Poly IIs) use the cccDNA as a template to produce viral RNAs, such as pgRNA, L, S, PreC, and X mRNAs and, the viral proteins are synthesized by ribosomes through the translation of mRNAs. Polymerase and pgRNA form a 1:1 complex called a Ribonucleoprotein (RNP) complex [7]. The nucleocapsid is formed by encapsulating this RNP complex by C proteins and it is commonly known as the immature nucleocapsid. The pgRNA is reverse-transcribed by polymerase [8], resulting in the immature nucleocapsid being converted into a rcDNA-containing nucleocapsid, known as the mature nucleocapsid [9]. This newly produced rcDNA-containing nucleocapsid will either return to the nucleus or be released as complete HBV from the infected hepatocytes [10]. A portion of rcDNA-containing capsids is transported again into the nucleus to increase the amount of supercoiled cccDNA. It is known as recycling of rcDNA-containing capsids [7] and is considered as a significant factor responsible for the intracellular dynamics of HBV replication.

In Literature, there are several viral dynamic models [11–16] proposed during the last two decades. Some of these are associated with HBV infection. These models are useful in understanding the pathogenesis of infection as well as devising better treatment protocols. Nowak et al. [17] analyzed a basic HBV infection model comprised of three compartments: uninfected hepatocytes, infected hepatocytes, and virions. Wodraz et al. [18] improved the basic model by including the effects of cytotoxic T cells and antibodies. By putting a standard incidence function in the place of mass action term of the uninfected hepatocytes and viruses, Min et al. [21] and Chen et al. [22] modified the classic viral infection model [17]. According to them the mass action term is not rational for the HBV infection as it implies that someone with a smaller liver is unlikely to be infected. In addition to the standard incidence function, the time delay during the production process of the virus was also taken into account by Gourley et al. [23]. Rather than using constant growth terms, Hews et al. [24] introduced a modified model that considers the logistic growth of uninfected hepatocytes. Eikenberry et al. [20] presented a delay model on HBV infection when uninfected hepatocytes proliferated logistically. Haug et al. [25] proposed a new model using another incidence function, called Beddington-DeAngelis type incidence function. Yu Ji et al. [26] first showed that the effects of immune response is not constant, and it follows a periodic function. The cure rate of the infected hepatocytes is an important factor in viral infection. Wang et al. [19] extended the model of Min et al. [21] by incorporating the effects of cure rate of infected hepatocytes. Fatehi et al. [27] determined that in HBV infection, NK cell takes a significant role in apoptosis as it kills the infected cell by producing the perforin and granzymes. Using a mathematical model that incorporates intracellular components of HBV infection, Murray et al. [8] were able to estimate the infection dynamics and clearance of viruses in three chimpanzees who were acutely infected. Murray et al. [28] proposed another mathematical model with three compartments and measured the half-life of HBV as approximately four hours. This model was modified by considering the uninfected hepatocytes and also studied with delay differential equation by Manna and Chakrabraty [30]. Considering the effects of antibodies and CTLs, Danane et al. [31] extended the model proposed by Manna and Chakrabraty [30], including CTL immune response and examined the optimality of the model. Using an average incidence rate, Guo et al. [32] established the global stability of a delayed-diffusive HBV infection model. Fatehi et al. [7] built up an Intracellular model of HBV infection and compared various kinds of therapeutic strategies. An important biological indicator of virus dynamics is the age of the infected cells. Recently, Liu et al. [33] proposed an age-structured model of HBV that treated HBV capsids as a separate compartment. There are mainly two roots of infection spread: virus-to-cell and cell-to-cell transmission.

In some recent biological studies [9, 10, 34], it is observed that the severity of HBV infection are greatly affected by the recycling of HBV DNA-containing capsids but how this recycling of HBV capsids contributes to the virus replication is poorly understood. One of the reason could be the increase in number of viruses in the liver, since a portion of newly produced capsids that are eventually reused as core particles providing an additional source for supercoiled cccDNA. In order to control HBV transmission in host, having a clear knowledge on recycling of capsids is extremely important. Although some mathematical studies have been conducted on HBV transmission in a host, only a few of them considered the HBV DNA-containing capsids as a separate compartment. However, these models failed to capture the actual dynamics of HBV infection. The main reason for this failure could be ignoring the recycling effects

of capsids. In this study, an improved mathematical model incorporating the recycling effects of HBV capsids is proposed for the first time. This model is expected to reveal the HBV intracellular dynamics more realistically compared to already available models. In a nutshell, we have mainly concentrated on the following things:

- (i) The effects of recycling of capsids in the HBV infection.
- (ii) The effects of volume fraction of capsids on the disease dynamics.
- (iii) Global sensitivity analysis of model parameters using the method Latin hypercube sampling (LHS)-Partial rank correlation coefficient (PRCC).

1 Mathematical model

The persistence of HBV infection for a long period in patients depends on the stability of cccDNA in the infected hepatocytes. cccDNA plays a central role in disease progression. There are two main sources of cccDNA: HBV DNA-containing capsids produced directly from the incoming virus from extracellular space and HBV DNA-containing capsids produced within the hepatocytes by recycling [7, 9, 34]. The recycling of capsids is not a continuous process. Depending on the availability of viral surface proteins (L, M, S), a portion of newly produced HBV DNA-containing capsids goes back to the nucleus to amplify the pool of cccDNA. So, the volume fraction of capsids in favor of virus production is generally a function of the surface protein (L, M, S). Assume that $\alpha \in (0, 1)$ be the volume fraction of capsids in favour of virus production, then α is a function of surface proteins. However, a fixed estimated value of α is used throughout the study for simulation purposes. Accordingly, the proposed model is described by the system of ordinary differential equations following:

$$\begin{aligned}
 \text{Susceptible hepatocytes :} & \quad \frac{dX}{dt} = \lambda - \mu X - kVX, \\
 \text{Infected hepatocytes:} & \quad \frac{dY}{dt} = kVX - \delta Y, \\
 \text{HBV DNA-containing capsids:} & \quad \frac{dD}{dt} = aY + \gamma(1 - \alpha)D - \alpha\beta D - \delta D, \\
 \text{Viruses:} & \quad \frac{dV}{dt} = \alpha\beta D - cV.
 \end{aligned} \tag{1}$$

Here, $X(t), Y(t), D(t)$ and $V(t)$ denote the numbers of susceptible hepatocytes, infected hepatocytes, HBV DNA-containing capsids, and free viruses respectively. All the parameters $\mu, k, \delta, a, \alpha, \beta, \gamma$ and c are non-negative. In this model, λ is assumed to be constant growth rate of susceptible hepatocytes, and μ is their natural death rate. The usual death rate of infected hepatocytes, as well as capsids is δ . The parameter k describes rate at which the susceptible hepatocytes are infected by the viruses. HBV capsids are produced at the rate a from infected hepatocytes, and β denotes the production rate of new viruses. Here, c is the virus clearance rate, and capsids reproduce themselves by recycling at rate γ . In Figure 1, the diagrammatic representation of the system (1) is shown.

This paper is organized as follows. In Section 2, we prove that our proposed model is well-posed by showing the existence, uniqueness, non-negativity, and boundedness of the solutions of the system (1). In Section 3, we calculate the basic reproduction number and determine the existence of all steady states. We also establish the local stability of both steady states using Routh Hurwitz criteria and global stability by constructing the appropriate Lyapunov functional and Lyapunov-LaSalle invariance principle in this section. In Section 6, we discuss some numerical results which support our analytical theory. In Section 7, the proposed model is compared to the existing one, and the effects of some model parameters is analyzed by sensitivity analysis. We study the global sensitivity analysis of model parameters in section 8. Finally, a brief conclusion is provided in Section 9.

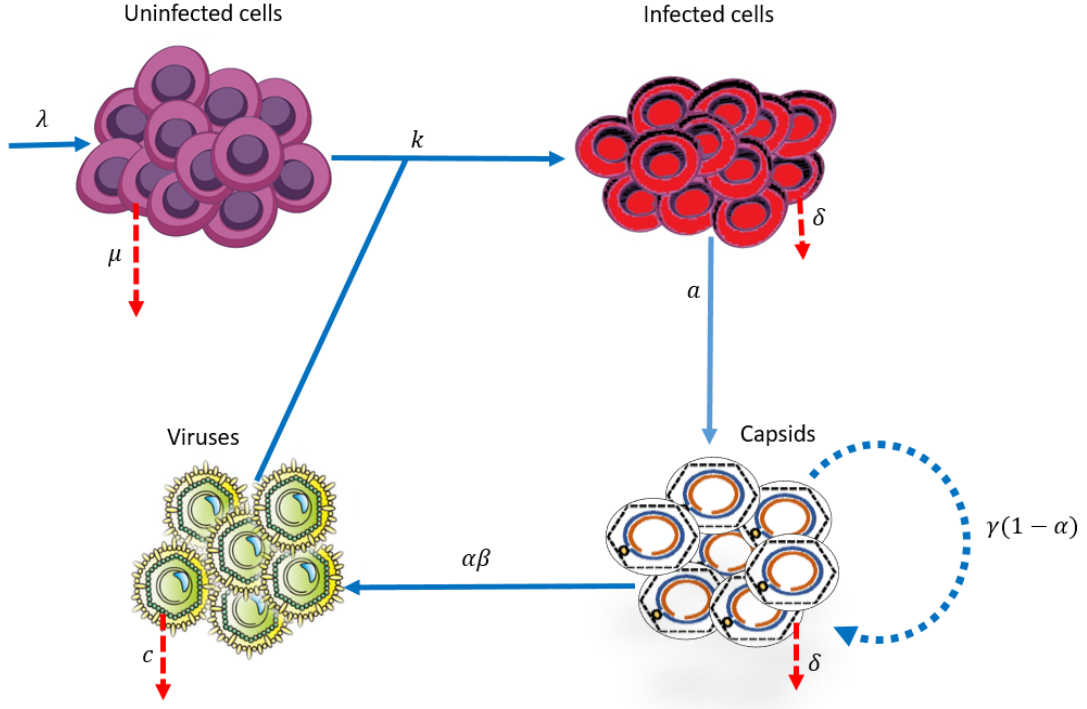


Figure 1: The diagrammatic representation of the system (1).

Uninfected Hepatocytes	Infected Hepatocytes	HBV DNA-containing Capsids	Hepatitis B Virus	Capsid-to-capsid Production Rate	Volume fraction HBV DNA-containing of capsids	References
✓	✓	✗	✓	✗	✗	[17]
✗	✓	✓	✓	✗	✗	[28]
✓	✓	✓	✓	✗	✗	[30, 33, 35]
✓	✓	✓	✓	✓	✓	Present work

Table 1: Comparison between present work and some previously existing studies based on various factors.

2 Properties of the solutions

Here, the existence and uniqueness of the solution for the system (1) are discussed. In order to ensure the feasibility of the model from biological point of view, it is crucial to show that all solutions remain non-negative and bounded across all non-negative initial conditions. The rationale behind this is that the number of cells or viruses must not drop below zero or exhibit limitless growth after the time of infection. Accordingly, the subsequent discussion confirms the non-negativity and boundedness of the solution.

2.1 Existence and uniqueness of the solutions

Each function of the right hand side of system (1) is polynomial functions of four variables $X(t)$, $Y(t)$, $D(t)$, $V(t)$. So, each function is continuous and satisfies Lipschitz's condition on any closed interval $[0, \eta]$, $\eta \in \mathbb{R}^+$, set of all positive real numbers. Therefore, the solution of the system (1) exists and is unique.

2.2 Non-negativity of the solutions

Theorem 1. *Under any non-negative initial conditions ($X(0) \geq 0$, $Y(0) \geq 0$, $D(0) \geq 0$, $V(0) \geq 0$), all solutions of the system (1) will remain non-negative.*

The proof of this theorem is presented in Appendix A.

2.3 Boundedness of the solutions

Theorem 2. For any non-negative initial condition ($X(0) \geq 0, Y(0) \geq 0, D(0) \geq 0, V(0) \geq 0$), the solutions of the system (1) are bounded for all $t > 0$, provided $R_s := \alpha\beta - (1 - \alpha)\gamma + \delta > 0$.

Proof. In this section, it is shown that the solutions for any non-negative initial condition should be bounded. For this purpose, a new variable $T(t)$ is introduced as,

$$T(t) = X(t) + Y(t).$$

Then, $\frac{dT}{dt} = \lambda - \mu X - \delta Y$. Define $\rho = \min\{\mu, \delta\}$. Then we have,

$$\frac{dT}{dt} \leq \lambda - \rho(X + Y) \implies \frac{dT}{dt} \leq \lambda - \rho T,$$

which implies that $\limsup_{t \rightarrow \infty} T(t) \leq \frac{\lambda}{\rho}$. This shows that $\limsup_{t \rightarrow \infty} X(t) \leq \frac{\lambda}{\rho}$ and $\limsup_{t \rightarrow \infty} Y(t) \leq \frac{\lambda}{\rho}$. So, $X(t)$ and $Y(t)$ are bounded for all $t > 0$. Now, from the third equation of the system (1), one can get

$$\frac{dD}{dt} \leq \frac{a\lambda}{\rho} + (\gamma(1 - \alpha) - \alpha\beta - \delta)D \implies \limsup_{t \rightarrow \infty} D(t) \leq \frac{a\lambda}{\rho(\alpha\beta + \delta - \gamma(1 - \alpha))},$$

provided $\alpha\beta - (1 - \alpha)\gamma + \delta > 0$.

Therefore, $D(t)$ is bounded for all $t > 0$. Using the boundedness of $D(t)$, from the last equation of the system (1) one can find

$$\begin{aligned} \frac{dV}{dt} &\leq \frac{a\lambda\alpha\beta}{\rho(\alpha\beta + \delta - \gamma(1 - \alpha))} - cV, \\ \implies \limsup_{t \rightarrow \infty} V(t) &\leq \frac{a\lambda\alpha\beta}{\rho c(\alpha\beta + \delta - \gamma(1 - \alpha))}. \end{aligned}$$

Hence, $V(t)$ is bounded for all $t > 0$. Therefore, all the population ($X(t), Y(t), D(t)$ & $V(t)$) are bounded. Consequently, one can also observe the closed, bounded, and positively invariant set as follows:

$$\mathcal{D} = \left\{ \left(X(t), Y(t), D(t), V(t) \right) \in \mathbb{R}_+^4 : 0 \leq X(t) + Y(t) \leq \frac{\lambda}{\rho}, \right. \\ \left. 0 \leq D(t) \leq \frac{a\lambda}{\rho(\alpha\beta + \delta - \gamma(1 - \alpha))}, 0 \leq V(t) \leq \frac{a\lambda\alpha\beta}{\rho c(\alpha\beta + \delta - \gamma(1 - \alpha))} \right\}$$

□

Remark 1. The condition $R_s > 0 \implies \alpha\beta - (1 - \alpha)\gamma + \delta > 0 \implies \gamma < \frac{\alpha\beta + \delta}{1 - \alpha}$. If γ meets this condition, then $D(t)$ becomes always bounded. Otherwise, $D(t)$ diverges to positive infinite i.e. the severity of infection increases significantly and situation of the patient becomes worse and worse with time. This relationship between these four parameters is very important when treating HBV patients.

Results

3 Existence and stability of equilibria

Before proceeding to the detailed study, it is mentioned that the condition $R_s > 0$ will be used throughout the further study.

3.1 Existence of equilibria

In order to evaluate the equilibrium points of the system (1), one need to consider the zero growth isoclines and their points of intersection. Thus, the equilibrium points of the system (1) are found by solving the system of equations

$$\begin{aligned}\lambda - \mu X - kVX &= 0, \\ kVX - \delta Y &= 0, \\ aY + \gamma(1 - \alpha)D - \alpha\beta D - \delta D &= 0, \\ \alpha\beta D - cV &= 0.\end{aligned}\tag{2}$$

It can be shown that the system (1) possesses two sets of equilibrium points.

- (i) **The uninfected steady-state or disease-free equilibrium (E_u):** The uninfected steady-state or disease-free equilibrium always exists, and it is denoted by $E_u = \left(\frac{\lambda}{\mu}, 0, 0, 0\right)$.
- (ii) **The infected steady-state or endemic equilibrium (E_i):** Mathematically, infected steady-state or endemic equilibrium points exists always. But biologically, the existence of this steady state depends on the basic reproduction number (R_0) and R_s (which is defined earlier). When $R_0 > 1$, and $R_s > 0$, the endemic equilibrium (E_i) occurs and is given by $E_i = (X_1, Y_1, D_1, V_1)$, where

$$\begin{aligned}X_1 &= \frac{c\delta(\alpha(\beta + \gamma) - \gamma + \delta)}{a\alpha\beta k}, & Y_1 &= \frac{a\alpha\beta k\lambda - c\delta\mu(\alpha(\beta + \gamma) - \gamma + \delta)}{a\alpha\beta\delta k}, \\ D_1 &= \frac{a\alpha\beta k\lambda - c\delta\mu(\alpha(\beta + \gamma) - \gamma + \delta)}{\alpha\beta\delta k(\alpha(\beta + \gamma) - \gamma + \delta)}, & V_1 &= \frac{a\alpha\beta k\lambda - c\delta\mu(\alpha(\beta + \gamma) - \gamma + \delta)}{c\delta k(\alpha(\beta + \gamma) - \gamma + \delta)}.\end{aligned}$$

3.2 Basic reproduction number (R_0)

In case of viral infection, the basic reproduction number is the number of secondary infective cells produced by a single infective cell, which is introduced into a fully susceptible population [36]. The first equation of the system (1) is for the uninfected class and the last three equations are meant for the infected class. The next-generation approach [37,38] is used to determine the basic reproduction number. Rewrite the last three equations of system (1) as,

$$\begin{aligned}\frac{dY}{dt} &= \mathcal{F}_1 - \mathcal{V}_1 \text{ where } \mathcal{F}_1 = kVX \text{ and } \mathcal{V}_1 = \delta Y, \\ \frac{dD}{dt} &= \mathcal{F}_2 - \mathcal{V}_2 \text{ where } \mathcal{F}_2 = 0 \text{ and } \mathcal{V}_2 = -aY - \gamma(1 - \alpha)D + \alpha\beta D + \delta D, \\ \frac{dV}{dt} &= \mathcal{F}_3 - \mathcal{V}_3 \text{ where } \mathcal{F}_3 = 0 \text{ and } \mathcal{V}_3 = -\alpha\beta D + cV.\end{aligned}\tag{3}$$

We define

$$\mathcal{F} = \begin{bmatrix} \frac{\partial \mathcal{F}_1}{\partial Y} & \frac{\partial \mathcal{F}_1}{\partial D} & \frac{\partial \mathcal{F}_1}{\partial V} \\ \frac{\partial \mathcal{F}_2}{\partial Y} & \frac{\partial \mathcal{F}_2}{\partial D} & \frac{\partial \mathcal{F}_2}{\partial V} \\ \frac{\partial \mathcal{F}_3}{\partial Y} & \frac{\partial \mathcal{F}_3}{\partial D} & \frac{\partial \mathcal{F}_3}{\partial V} \end{bmatrix}_{E_u} \quad \text{and} \quad \mathcal{V} = \begin{bmatrix} \frac{\partial \mathcal{V}_1}{\partial Y} & \frac{\partial \mathcal{V}_1}{\partial D} & \frac{\partial \mathcal{V}_1}{\partial V} \\ \frac{\partial \mathcal{V}_2}{\partial Y} & \frac{\partial \mathcal{V}_2}{\partial D} & \frac{\partial \mathcal{V}_2}{\partial V} \\ \frac{\partial \mathcal{V}_3}{\partial Y} & \frac{\partial \mathcal{V}_3}{\partial D} & \frac{\partial \mathcal{V}_3}{\partial V} \end{bmatrix}_{E_u},$$

where E_u denotes the disease-free equilibrium point which is calculated above. After simplification, we get

$$\mathcal{F} = \begin{bmatrix} 0 & 0 & \frac{k\lambda}{\mu} \\ 0 & 0 & 0 \\ 0 & 0 & 0 \end{bmatrix} \quad \text{and} \quad \mathcal{V} = \begin{bmatrix} \delta & 0 & 0 \\ -a & -\gamma(1 - \alpha) + \alpha\beta + \delta & 0 \\ 0 & -\alpha\beta & c \end{bmatrix}.$$

The basic reproduction number of the system (1) is defined by $R_0 = \rho(\mathcal{F}\mathcal{V}^{-1})$, where $\rho(\mathcal{F}\mathcal{V}^{-1})$ is defined as the spectral radius of the matrix $\mathcal{F}\mathcal{V}^{-1}$, which is given by $R_0 = \frac{ak\lambda\alpha\beta}{(c\alpha\beta\delta - c\gamma\delta + c\alpha\gamma\delta + c\delta^2)\mu}$.

3.3 Stability analysis of equilibria

3.3.1 Local stability analysis

Theorem 3. *The disease-free equilibrium E_u is locally asymptotically stable when $R_0 < 1$ and $R_s > 0$.*

Proof. The Jacobian matrix of the system (1) at the disease-free steady state (E_u) is given by

$$\begin{bmatrix} -\mu & 0 & 0 & -\frac{k\lambda}{\mu} \\ 0 & -\delta & 0 & \frac{k\lambda}{\mu} \\ 0 & a & \gamma(1-\alpha) - \alpha\beta - \delta & 0 \\ 0 & 0 & \alpha\beta & -c \end{bmatrix}. \quad (4)$$

It is clear that $-\mu$ is a negative eigenvalue of the Jacobian matrix (4). The other three eigenvalues of the Jacobian matrix (4) are the eigenvalues of the matrix

$$\begin{bmatrix} -\delta & 0 & \frac{k\lambda}{\mu} \\ a & \gamma(1-\alpha) - \alpha\beta - \delta & 0 \\ 0 & \alpha\beta & -c \end{bmatrix}. \quad (5)$$

By using the Routh-Hurwitz criteria [39], it is shown that all eigenvalues of the matrix (5) are either negative or have negative real parts. Let the characteristic equation of this matrix (5) be

$$x^3 + A_1x^2 + A_2x + A_3 = 0.$$

When $R_0 < 1$ and $R_s > 0$,

$$\begin{aligned} A_1 &= R_s + c + \delta > 0, \\ A_2 &= (\delta + c)R_s + c\delta > 0, \\ A_3 &= -\frac{a\alpha\beta k\lambda}{\mu} + \alpha\beta c\delta - (1-\alpha)c\gamma\delta + c\delta^2, \\ &= -\frac{a\alpha\beta k\lambda}{\mu} + c\delta R_s > 0, \\ A_1A_2 - A_3 &= (R_s + c + \delta)((\delta + c)R_s + c\delta) + \frac{a\alpha\beta k\lambda}{\mu} - c\delta R_s, \\ &= R_s(R_s + c + \delta)(c + \delta) + c\delta(c + \delta) + \frac{a\alpha\beta k\lambda}{\mu} > 0. \end{aligned}$$

Thus, the Routh-Hurwitz criteria is satisfied. Therefore, local asymptotically stability of the disease-free equilibrium is established when $R_0 < 1$. In case of $R_0 = 1$, it is seen that the determinant of Jacobian matrix (4) become zero and consequently it has at least one zero eigenvalue, and also when $R_0 > 1$, the matrix (4) has at least one positive eigenvalue and thus the disease-free equilibrium point will be unstable. \square

Theorem 4. *The endemic equilibrium E_i is locally asymptotically stable when the basic reproduction number $R_0 > 1$ and does not exist if $R_0 < 1$.*

Proof. The Jacobian matrix at the equilibrium E_i is

$$\begin{bmatrix} -\mu - kV_1 & 0 & 0 & -kX_1 \\ kV_1 & -\delta & 0 & kX_1 \\ 0 & a & \gamma(1-\alpha) - \alpha\beta - \delta & 0 \\ 0 & 0 & \alpha\beta & -c \end{bmatrix}.$$

The characteristic equation of the Jacobian matrix is given by

$$\begin{aligned} (-c-x)(\delta\mu + \delta kV_1 + kV_1x + x^2 + \delta x + \mu x)(-\alpha\beta - \alpha\gamma + \gamma - \delta - x) \\ -\alpha\beta(akxX_1 + ak\mu X_1) = 0. \end{aligned}$$

Comparing above equation with this equation $x^4 + B_1x^3 + B_2x^2 + B_3x + B_4 = 0$, we have

$$\begin{aligned} B_1 &= R_s + (c + \delta + kV_1 + \mu) > 0, \\ B_2 &= R_s(\delta + kV_1 + \mu + c) + kV_1(c + \delta) + \delta(c + \mu) + \mu > 0, \\ B_3 &= \frac{ak\lambda\alpha\beta(R_s(c + \delta) + c\delta)}{R_sc\delta} > 0, \\ B_4 &= a\alpha\beta k\lambda - R_sc\delta\mu > 0, \\ B_1B_2 - B_3 &= k^2V_1^2(R_s + \delta) + (R_s + \delta)(R_s + \delta + \mu)(\delta + \mu) + c^2(R_s + kV_1 + \delta + \mu) \\ &\quad + c(R_s + kV_1 + \delta + \mu) + k(aX_1\alpha\beta + V_1(R_s + \delta)(R_s + \delta + 2\mu)) > 0, \\ B_1B_2B_3 - B_3^2 - B_1^2B_4 &= a^3\alpha^3\beta^3k^3\lambda^3(R_s + c)(R_s + \delta)(c + \delta) + R_s^4c^4\delta^4\mu(R_s + c + \delta)^2 \\ &\quad + a\alpha R_s^2\beta c^2\delta^2k\lambda(R_s + c + \delta)\left(R_s^2(c^2 + c\delta + \delta^2) + R_sc\delta(c + \delta + 2\mu) + c^2\delta^2\right) \\ &\quad + a^2\alpha^2R_s\beta^2c\delta k^2\lambda^2\left(R_s^3(c + \delta) + R_s^2(2c^2 + 3c\delta + 2\delta^2) + R_sc\delta\mu + (c + \delta)^3\right) \\ &\quad + c\delta(c + \delta)^2 > 0. \end{aligned}$$

So, B_1 , B_2 , B_3 , and B_4 satisfy all the conditions of Routh-Hurwitz criteria when $R_0 > 1$ and $R_s > 0$. Thus, all the eigenvalues of the matrix are either negative or have negative real parts. Therefore, the endemic equilibrium is locally asymptotically stable. \square

3.3.2 Global stability analysis

In order to prove the global stability of equilibria, Theorem 7.1 of the book [39] is used. Two suitable Lyapunov functions are defined as follows:

$$\begin{aligned} \mathcal{L}_1(t) &= X_0 \left(\frac{X(t)}{X_0} - 1 - \ln \left(\frac{X(t)}{X_0} \right) \right) + Y(t) + \frac{\delta}{a}D(t) + \frac{\delta(-\gamma(1-\alpha) + \alpha\beta + \delta)}{a\alpha\beta}V(t). \\ \mathcal{L}_2(t) &= X_1 \left(\frac{X(t)}{X_1} - 1 - \ln \left(\frac{X(t)}{X_1} \right) \right) + Y_1 \left(\frac{Y(t)}{Y_1} - 1 - \ln \left(\frac{Y(t)}{Y_1} \right) \right) \\ &\quad + \frac{\delta D_1}{a} \left(\frac{D(t)}{D_1} - 1 - \ln \left(\frac{D(t)}{D_1} \right) \right) + \frac{\delta R_s V_1}{a\alpha\beta} \left(\frac{V(t)}{V_1} - 1 - \ln \left(\frac{V(t)}{V_1} \right) \right), \end{aligned}$$

Both functions are radially unbounded and globally positively definite. Therefore, the choices of Lyapunov functions are appropriate.

Theorem 5. *The disease-free equilibrium point E_u is globally asymptotically stable if $R_0 \leq 1$.*

Proof. To prove the asymptotic global stability of disease-free equilibrium point, the first Lyapunov function $\mathcal{L}_1(t)$ (defined above) is considered.

$$\mathcal{L}_1(t) = X_0 \left(\frac{X(t)}{X_0} - 1 - \ln \left(\frac{X(t)}{X_0} \right) \right) + Y(t) + \frac{\delta}{a}D(t) + \frac{\delta(-\gamma(1-\alpha) + \alpha\beta + \delta)}{a\alpha\beta}V(t).$$

Now,

$$\begin{aligned}
\frac{d\mathcal{L}_1(t)}{dt} &= X_0 \left(\frac{X'}{X_0} - \frac{X'}{X} \right) + Y'(t) + \frac{\delta}{a} D'(t) + \frac{\delta(-\gamma(1-\alpha) + \alpha\beta + \delta)}{a\alpha\beta} V'(t) \\
&= \left(1 - \frac{X_0}{X} \right) X'(t) + Y'(t) + \frac{\delta}{a} D'(t) + \frac{\delta(-\gamma(1-\alpha) + \alpha\beta + \delta)}{a\alpha\beta} V'(t) \\
&= \left(1 - \frac{X_0}{X(t)} \right) (\lambda - \mu X(t) - kV(t)X(t)) + kV(t)X(t) \\
&\quad + \frac{\delta}{a} (aY(t) + \gamma(1-\alpha) - \alpha\beta - \delta D) + \frac{\delta(-\gamma(1-\alpha) + \alpha\beta + \delta)}{a\beta} (\beta D - cV) \\
&= \lambda \left(2 - \frac{X}{X_0} - \frac{X_0}{X} \right) + \frac{a\alpha\beta k\lambda - c\delta\mu(-\gamma(1-\alpha) + \alpha\beta + \delta)}{a\alpha\beta\mu} V.
\end{aligned}$$

From the article of Kajiwara et al. [41], $\left(2 - \frac{X}{X_0} - \frac{X_0}{X} \right) \leq 0$ and since, $R_0 \leq 1$, $a\alpha\beta k\lambda - c\delta\mu(-\gamma(1-\alpha) + \alpha\beta + \delta) \leq 0$. Therefore, $\frac{d\mathcal{L}_1(t)}{dt} \leq 0$. We consider the largest invariant set $\mathcal{M}_1 = \left\{ (X, Y, D, V) \in \mathbb{R}^4 : \frac{d\mathcal{L}_1(t)}{dt} = 0 \right\}$.

The solution of the equation $\frac{d\mathcal{L}_1(t)}{dt} = 0$ is $\left(\frac{\lambda}{\mu}, 0, 0, 0 \right)$ only, which is the equilibrium point E_u . So, based on the Lyapunov-LaSalle invariance principle [39], the disease-free equilibrium point, E_u is globally asymptotically stable whenever $R_0 \leq 1$. \square

Theorem 6. *The endemic equilibrium E_i is globally asymptotically stable if $R_0 > 1$.*

Proof. We are approaching the problem by taking into account the second Lyapunov function $\mathcal{L}_2(t)$.

$$\begin{aligned}
\mathcal{L}_2(t) &= X_1 \left(\frac{X(t)}{X_1} - 1 - \ln \left(\frac{X(t)}{X_1} \right) \right) + Y_1 \left(\frac{Y(t)}{Y_1} - 1 - \ln \left(\frac{Y(t)}{Y_1} \right) \right) \\
&\quad + \frac{\delta D_1}{a} \left(\frac{D(t)}{D_1} - 1 - \ln \left(\frac{D(t)}{D_1} \right) \right) + \frac{\delta R_s V_1}{a\alpha\beta} \left(\frac{V(t)}{V_1} - 1 - \ln \left(\frac{V(t)}{V_1} \right) \right), \tag{6}
\end{aligned}$$

where R_s is defined above.

Differentiating (6) with respect to t , we have

$$\begin{aligned}
\frac{d\mathcal{L}_2(t)}{dt} &= X_1 \left(\frac{X'(t)}{X_1} - \frac{X'(t)}{X(t)} \right) + Y_1 \left(\frac{Y'(t)}{Y_1} - \frac{Y'(t)}{Y(t)} \right) \\
&\quad + \frac{\delta D_1}{a} \left(\frac{D'(t)}{D_1} - \frac{D'(t)}{D(t)} \right) + \frac{\delta R_s V_1}{a\alpha\beta} \left(\frac{V'(t)}{V_1} - \frac{V'(t)}{V(t)} \right) \\
&= \left(1 - \frac{X_1}{X(t)} \right) X'(t) + \left(1 - \frac{Y_1}{Y(t)} \right) Y'(t) + \frac{\delta D_1}{a} \left(1 - \frac{D_1}{D(t)} \right) D'(t) \\
&\quad + \frac{\delta R_s V_1}{a\alpha\beta} \left(1 - \frac{V_1}{V(t)} \right) V'(t) \\
&= -\mu X(t) \left(1 - \frac{X_1}{X(t)} \right)^2 + \delta Y_1 \left(4 - \frac{Y(t)D_1}{D(t)Y_1} - \frac{D(t)V_1}{D_1V(t)} - \frac{X(t)Y_1V(t)}{X_1Y(t)V_1} - \frac{X_1}{X(t)} \right).
\end{aligned}$$

$$\left[\text{Using } D_1 = \frac{a}{R_s} Y_1 \text{ and } V_1 = \frac{a\alpha\beta}{R_s c} Y_1 \right]$$

Clearly, the first term of the above equation is negative unless $X(t) = X_1$. To prove the negativity of the second term, define

$$x_1 = \frac{Y(t)D_1}{D(t)Y_1}, \quad x_2 = \frac{D(t)V_1}{D_1V(t)}, \quad x_3 = \frac{X(t)Y_1V(t)}{X_1Y(t)V_1}, \quad x_4 = \frac{X_1}{X(t)}.$$

It is clear that $x_i \geq 0$ for $i = 1, 2, 3, 4$ and $x_1 x_2 x_3 x_4 = 1$. Applying $A.M \geq G.M$,

$$\begin{aligned}
\frac{x_1 + x_2 + x_3 + x_4}{4} &\geq (x_1 x_2 x_3 x_4)^{\frac{1}{4}}, \\
\implies \frac{Y(t)D_1}{D(t)Y_1} + \frac{D(t)V_1}{D_1V(t)} + \frac{X(t)Y_1V(t)}{X_1Y(t)V_1} + \frac{X_1}{X(t)} &\geq 4.
\end{aligned}$$

Hence, $\frac{d\mathcal{L}_2(t)}{dt} \leq 0$ when $R_0 > 1$. Let the largest invariant set $\mathcal{M}_2 = \left\{ (X, Y, D, V) \in \mathbb{R}^4 : \frac{d\mathcal{L}_2(t)}{dt} = 0 \right\}$.

It is noticed that the solution of the equation $\frac{d\mathcal{L}_2(t)}{dt} = 0$ is only (X_1, Y_1, D_1, V_1) , which is the equilibrium point E_i . So, the endemic equilibrium point is globally asymptotically stable whenever $R_0 > 1$ based on the Lyapunov-LaSalle invariance principle. \square

4 Bifurcation Analysis

In this section, the bifurcation analysis of the proposed model (1) is performed. Stability criteria of E_0 indicates that E_0 will be stable if $\mu > \frac{ak\alpha\beta\lambda}{R_s c\delta}$ ($= \mu^*$), otherwise it will be unstable *i.e.* the stability of E_0 changes as μ crosses the threshold value $\mu = \mu^*$. On the other hand, the endemic equilibrium E_i (although E_i is not feasible in the context of biology) becomes unstable if $\mu > \mu^*$. Thus, the equilibrium points coincide and exchange their stability which leads to the transcritical bifurcation of the system (1) around the point E_0 at $\mu = \mu^*$ with natural death rate parameter μ as the bifurcation parameter. It is seen that the Jacobian matrix (4) has one zero eigenvalue when $\mu = \mu^*$. In order to verify the existence of transcritical bifurcation analytically, Sotomayor's theorem [40] is applied on the system (1) around the disease-free equilibrium point E_0 when $\mu = \mu^*$. The R.H.S of system (1) can be represented in vector form as

$$f(X, Y, D, V) = \begin{pmatrix} \lambda - \mu X - kVX \\ kVX - \delta Y \\ aY + \gamma(1 - \alpha)D - \alpha\beta D - \delta D \\ \alpha\beta D - cV \end{pmatrix} \quad (7)$$

Differentiating the function $f(X, Y, D, V)$ partially with respect to μ , it is obtained that $f_\mu(X, Y, D, V) = (-X \ 0 \ 0 \ 0)^T$. The Jacobian matrix (4) at disease-free equilibrium point (E_0) and its transpose matrix have an eigenvalue $\xi = 0$ with eigenvectors

$$v = \begin{pmatrix} k\lambda & a\lambda & ak\lambda & 1 \end{pmatrix}^T \text{ and } w = \begin{pmatrix} 0 & \frac{a\alpha\beta}{\delta R_s} & \frac{\alpha\beta}{R_s} & 1 \end{pmatrix}^T.$$

Now, at E_0 we have verified the following transversality conditions:

$$(i) \ w^T f_\mu(E_0, \mu^*) = \begin{pmatrix} 0 & \frac{a\alpha\beta}{\delta R_s} & \frac{\alpha\beta}{R_s} & 1 \end{pmatrix} \begin{pmatrix} -\lambda & 0 & 0 & 0 \end{pmatrix}^T = 0$$

$$(ii) \ w^T [Df_\mu(E_0, \mu^*)v] = -\frac{k\lambda}{\mu^2} \neq 0$$

$$(iii) \ w^T [D^2 f(E_0, \mu^*)(v, v)] = -\frac{2\alpha\beta k^2 \lambda}{R_s \delta \mu^2} \neq 0$$

All the notations used here are same as in the book of Lawrence Perko [40]. Therefore, all three conditions of Sotomayor's theorem hold and the system (1) undergoes transcritical bifurcation at E_0 as the natural death rate of uninfected hepatocytes μ , crosses the threshold value μ^* .

5 Parameter estimation and model calibration

In this section, in order to enhance the realism of viral dynamics and to improve the reliability of our robust predictions, the proposed model is calibrated using experimental data collected from the previously published article of Asabe et al. [29]. In their research, Asabe et al. examined the effects of varying inoculum sizes on the kinetics of viral spread and immune system in a cohort of nine young, healthy chimpanzees. In adherence to ethical guidelines, handling procedures of all animals were carried out with the sole intention of human use. It was observed that the viral load for six out of nine chimpanzees reached a peak level of 2×10^{10} within three weeks from the time of inoculation. Later, the virion load decreased within 15 weeks and reached below the detection level. On the other hand, this experiment also

Table 2: Estimation of parameters.

Parameters	Descriptions Values	Estimated value (Baseline value)	Units
λ	Constant growth rate of uninfected hepatocytes	2.67×10^7	cells ml ⁻¹ day ⁻¹
μ	Natural death rate of uninfected hepatocyte	0.096	day ⁻¹
k	Virus-to-cell infection rate	3.38×10^{-12}	ml virion ⁻¹ day ⁻¹
a	Production rate of capsid from infected hepatocyte	157	capsids cell ⁻¹ day ⁻¹
β	Production rate of virus from capsid	1.83	day ⁻¹
δ	Death rate of infected hepatocyte & capsid	0.24	day ⁻¹
c	Death rate of virus	3.93	day ⁻¹
α	Volume fraction of HBV DNA-containing capsid	0.84	unitless
γ	Capsid to capsid production rate recycling rate of capsids	1.24	day ⁻¹

documented that the remaining three chimpanzees developed chronic infection. The concentration of HBV DNA of these three chimpanzees (1603, 1616, A2A007) who persisted infection and another chimpanzee (1618) which developed acute infection are considered in order to estimate the model parameters and validate our model. In each case, the model parameters are estimated by minimizing the sum-of-squares error (SSE) which is given by

$$SSE = \sum_{i=1}^n (P_i - p(i))^2, \quad (8)$$

where P_i and $p(i)$ denote the experimental data and model solution, respectively. Four sets of parameters' values are obtained for four chimpanzees. For further analysis of the system (1) and numerical simulation, the average value of each parameter will be used throughout the study. The average values of parameters are given in Table 2. In addition, the estimated parameter values are compared with the existing values in the literature [28, 42], and it is seen that there is no significant disparities between the two sets of values.

In Figure 2, the experimental data and solution of the proposed model are compared. It is observed that for all four chimpanzees, the proposed model effectively captures the infection dynamics. Although the model solution agrees well with the experimental data, there are some discrepancies. The possible reasons for this could be that many crucial factors of virus dynamics such as the roles of immune system, intracellular delay are neglected in the proposed model.

Discussion

6 Numerical simulation

From our theoretical results it is seen that R_0 and R_s are two crucial threshold numbers for the dynamics of HBV infection. Here, we numerically study the stability of the model for different values of R_0 . The numerical simulation examines the asymptotic behavior of the system (1) for different cases. The system (1) is solved numerically and the results are plotted graphically. We utilize the value of parameters from Table 2. In this context, we consider three different initial conditions, as $ic_1 = (2.56 \times 10^8, 0.99 \times 10^8, 1.60 \times 10^{10}, 0.369 \times 10^{10})$, $ic_2 = (7.68 \times 10^8, 2.97 \times 10^8, 4.82 \times 10^{10}, 1.10 \times 10^{10})$ and $ic_3 = (12.79 \times$

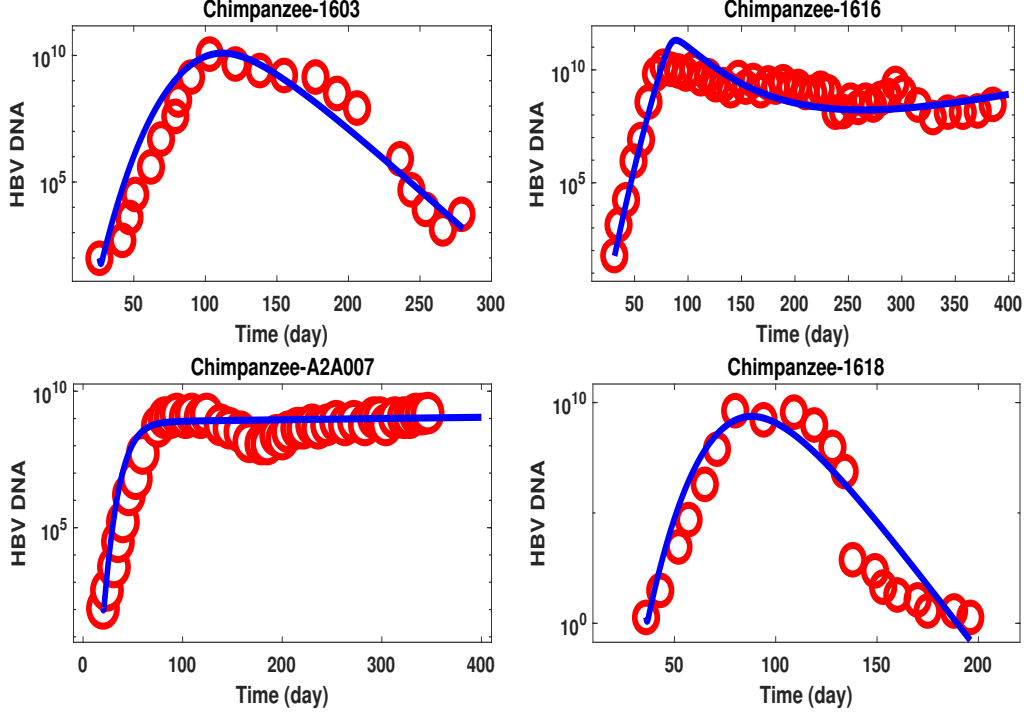


Figure 2: Experimental validation of the model. The experimental data is represented by red circles, while the solid blue line corresponds to the numerical solution of the system (1).

$10^8 4.95 \times 10^8, 8.04 \times 10^{10}, 1.85 \times 10^{10}$). In addition, two sets of parameters are chosen, the first one provides $R_0 < 1$, and the second one leads to $R_0 > 1$.

6.1 Disease free equilibrium

In order to examine the disease dynamics for $R_0 < 1$, the value of k is different from Table 2, namely $k = 3 \times 10^{-13}$ [?], is chosen while the values of other parameters remain unchanged. The resulting dynamics is represented in Figure 3. Consider the duration of the simulation as 500 days. For each initial condition, the concentration level of uninfected hepatocytes increases gradually, and the concentration level of infected hepatocytes decreases with time before stabilizing to the disease-free equilibrium $E_u = (2.6 \times 10^9, 0, 0, 0)$ at around $t = 400$. Moreover, the dynamics of HBV DNA-containing capsids and virions is something different. Initially, both concentrations of capsids and virions increase progressively, reach the peak level, then decrease continuously and approach zero. Therefore, the disease-free equilibrium is globally asymptotically stable, and this supports the theoretical result stated in Theorem 5. Additionally, this results also demonstrates the clearance of HBV infection in the presence of the effects of capsid recycling.

6.2 Endemic equilibrium ($R_0 > 1$)

In order to analyze the stability of endemic equilibrium numerically, we choose $k = 3 \times 10^{-12}$. The dynamics in this case are shown in Figure 4. It is seen that the concentration level of uninfected hepatocytes, infected hepatocytes, HBV DNA-containing capsids, and viruses initially oscillate for some time and slowly converge to the endemic equilibrium point asymptotically. Consequently, the numerical results agree with the theoretical results stated in Theorem 6.

7 Comparison of the model

In this section, it is demonstrated how the dynamics of the system (1) changes when the capsid-to-capsid production rate (γ) is included in the model.

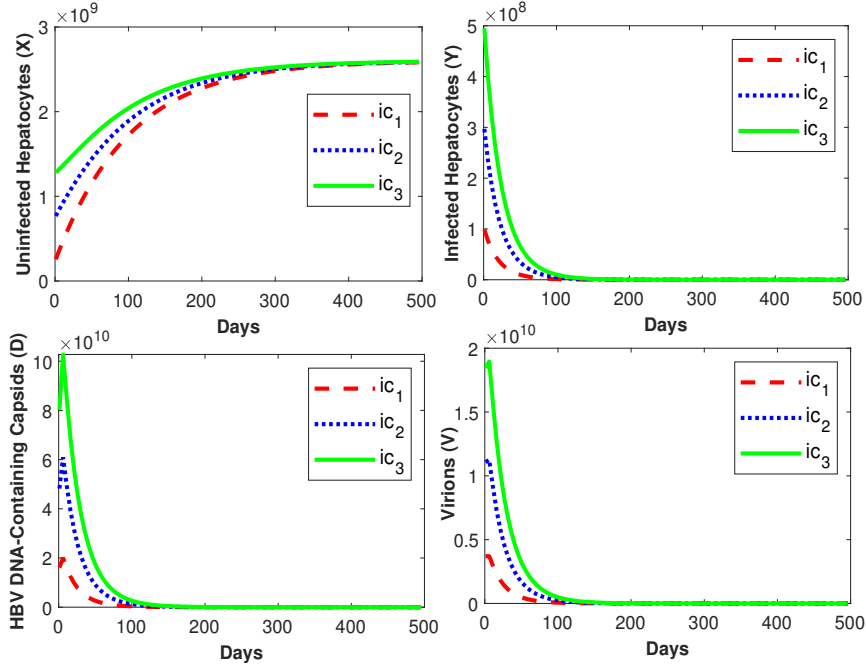


Figure 3: The dynamics of the system (1) while $R_0 < 1$ with three different initial states ic_1, ic_2, ic_3 .

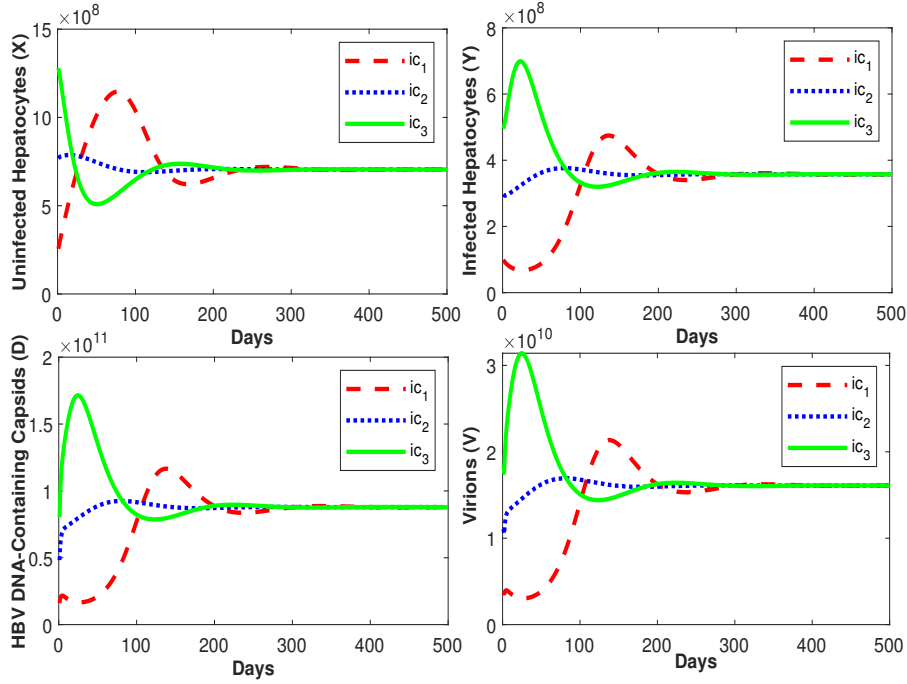


Figure 4: The dynamics of the system (1) while $R_0 > 1$ with three different initial states ic_1, ic_2, ic_3 .

- (i) **BMwoR**: Basic HBV model where the effects of “recycling” of HBV DNA-containing capsid is not considered. In this case $\gamma = 0$ and $0 < \alpha < 1$.
- (ii) **BMwR**: Basic HBV model where the effects of “recycling” of HBV DNA-containing capsid is considered. In this case $0 < \alpha < 1$, and $\gamma > 0$.

The variations in the concentration level of uninfected hepatocytes, infected hepatocytes, HBV capsids, and viruses are presented in Figure 5. It is observed that when the effects of recycling of capsids is incorporated in the model, the equilibria remains stable, but the stability level of uninfected hepatocytes decreases significantly, whereas the stability levels of infected hepatocytes, HBV DNA-containing capsids, and virions increase in large amount. So, Figure 5 points out that the inclusion of recycling of capsids in the HBV model makes momentous differences in the dynamics of infection.

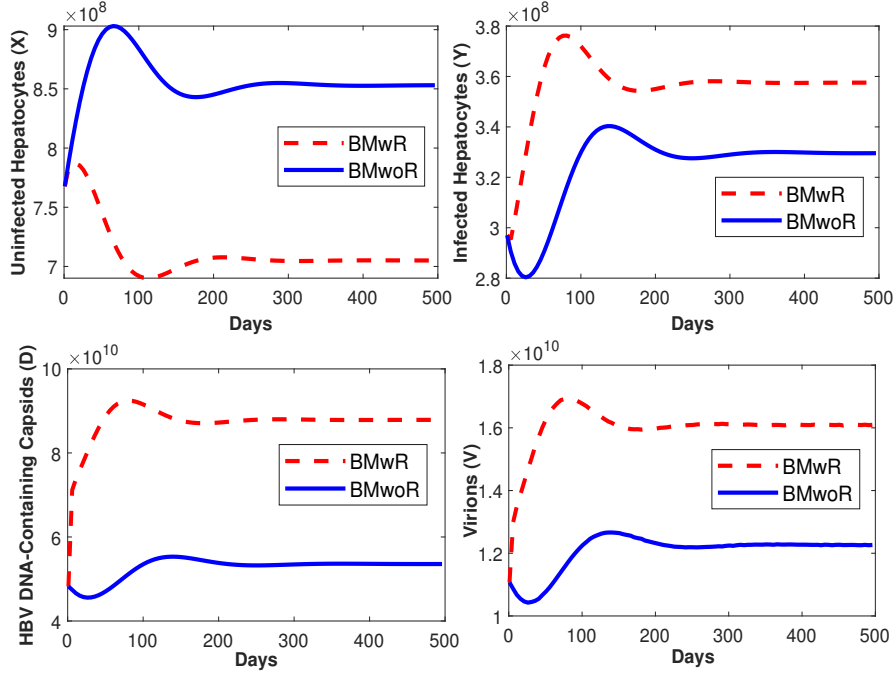


Figure 5: Comparison of model. The parameter values are taken from Table 2. Here (i) BMwoR: Basic model without recycling of capsid (ii) BMwR: Basic model with recycling of capsids.

7.1 Effects of volume fraction (α) of HBV DNA-containing capsids

The effects of volume fraction of capsids (α) on the system (1) are studied for two cases. In the first case, impacts of recycling of capsids on the system (1) are ignored, while in the second case, it is considered. In Figure 6, effects of α in the absence of recycling of capsids are demonstrated. The numerical simulation is performed for six values of α , namely, $\alpha = 0.5, 0.6, 0.7, 0.8, 0.9$ & 1.0 while keeping fixed the other parameters. The condition $R_s > 0$ is satisfied for every value of α . In all cases, $R_0 > 1$ *i.e.* the system converges to corresponding endemic equilibrium points. Figure 6 shows that the uninfected hepatocytes and HBV capsids decline, but infected hepatocytes and viruses progressively increase while α increases.

However, when the recycling effects of capsids are included in the model, the reverse results are seen for uninfected, infected hepatocytes, and viruses in Figure 7. There is no change observed in the dynamics of capsids, but the stability level significantly increases for the same value of α . Consequently, when $\alpha = 1.0$ (in this case recycling of capsids is ignored), it is clear that the concentration level of uninfected hepatocytes is at a highest level while that of infected hepatocytes, HBV capsids, and viruses get stabilized at a lowest level. Thus, the results for these two cases are significantly different. The low value of volume fraction of capsids (α) implies that a less number of capsids can produce new viruses, and a large number of capsids get accumulated inside the hepatocytes. Therefore, an accumulation of core particles (capsids) within the infected hepatocytes can be a cause of severe infection rather than the rapidly release of viruses. Thus, the role of α cannot be ignored in the design of strategies for controlling HBV infection.

7.2 Effects of capsid to capsid production rate (γ)

In Figure 8, we present the impact of recycling rate or capsid-to-capsid production rate (γ) on all the four populations in the system (1). The parameter values are same as in Table 2 except γ . Six different values of γ ($= 0.5, 1.0, 1.5, 2.0, 2.5, 3.0$) are chosen for simulation in such a way that the criteria for boundedness of solution $R_s > 0$ is satisfied. For these value of parameters, the corresponding values of R_0 are greater than unity. The value of R_0 increases with increase of γ . Also, one more observation is seen that when γ takes its minimum value zero *i.e.* no capsid-to-capsid production rate is considered, system achieves its stability asymptotically with maximum concentration of uninfected hepatocytes and this concentration drops when γ rises. It may be noted that the concentration level of infected hepatocytes decreases with the increase in γ and attains its minimum value when $\gamma = 0$. A similar scenario is observed for the HBV DNA-containing capsids and virions. In other words, the peak level for the virus compartment

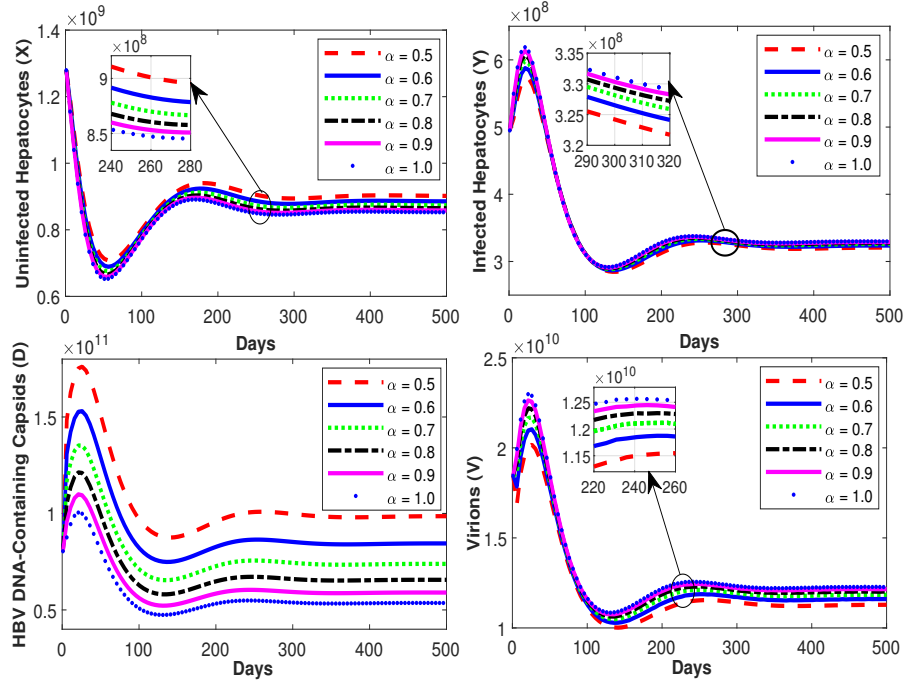


Figure 6: The effects of α on the dynamical system (1) in absence of recycling of capsids ($\gamma = 0$), and ic_3 is taken as the initial condition.

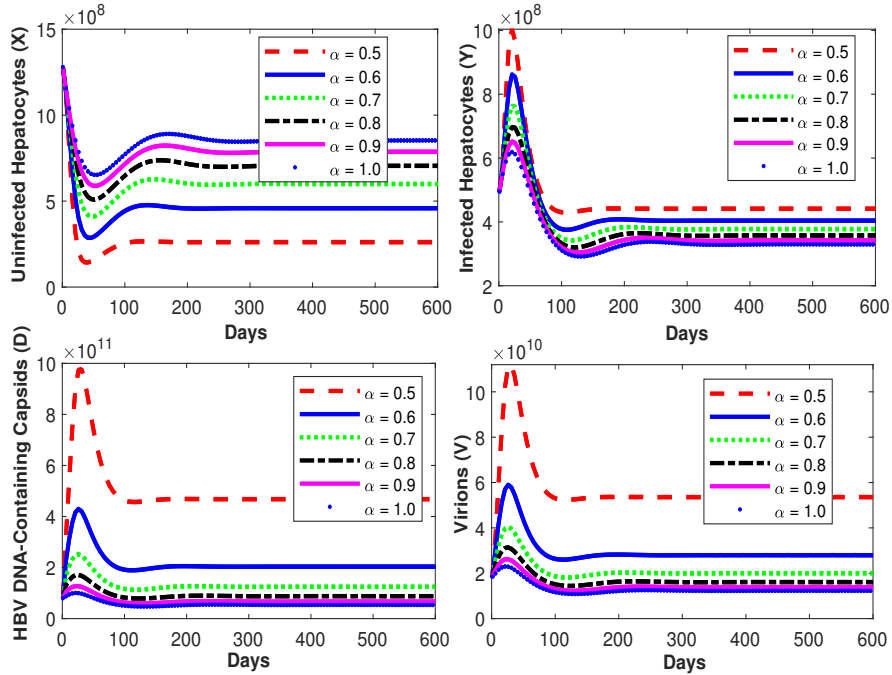


Figure 7: The effects of α on the dynamical system (1) when the effects of recycling of capsids is considered ($\gamma > 0$), and ic_3 is taken as the initial condition.

becomes smaller as γ decreases. Therefore, the severity of the infection becomes less and disappears faster. Biologically, one can see that for high value of γ , the situation becomes more critical for the patient, and it is difficult to be cured. So, this study indicates that the inclusion of capsid-to-capsid production rate in the model is crucial to study the dynamics of HBV infection in a more realistic way.

7.3 Effects of capsids to virus production rate (β)

For different values of β , the changes in dynamics of uninfected hepatocytes, infected hepatocytes, capsids, and viruses are shown in Figure 9. In this case, the effects of recycling of capsids are not taken into account. Six values of β ($=0.6, 0.7, 0.8, 0.9, 1.0, 1.1$) are considered keeping other parameters fixed as

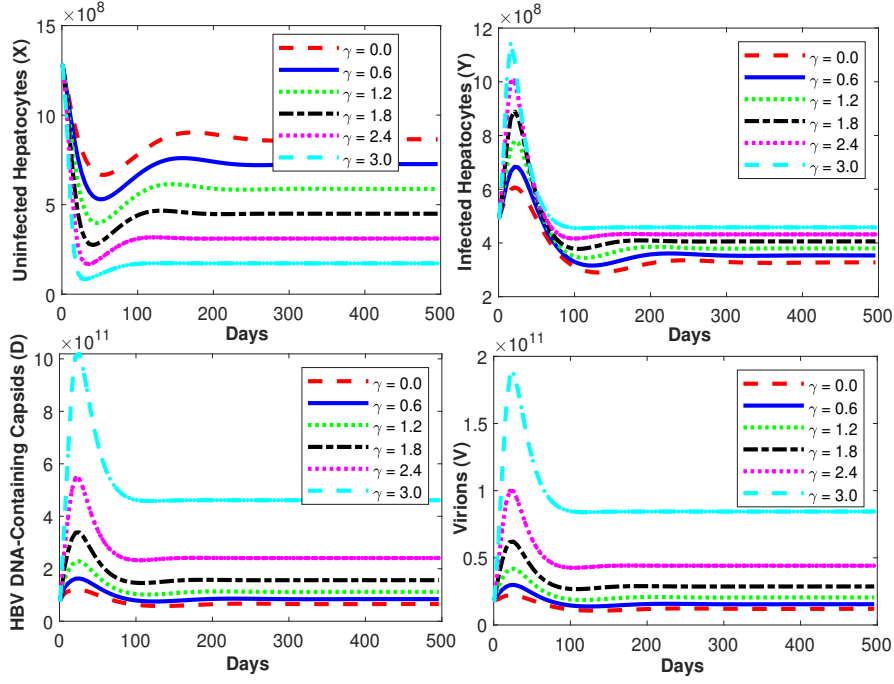


Figure 8: The effects of γ on the dynamical system (1) w.r.t the initial condition ic_3 .

shown in Table 2. For each value of β , $R_s > 0$ holds. When β decreases, the concentrations of uninfected hepatocytes and capsids increase, while opposite trends are observed for infected hepatocytes and viruses. For a low value of β , the amount of viruses (newly produced from the infected hepatocytes) also remains low.

On the other hand, the effects of recycling of capsids in the HBV dynamics reverse the impacts of β which is shown in Figure 10. If β decreases, concentration of uninfected hepatocytes increases whereas the numbers of infected hepatocytes, HBV DNA-containing capsids, and viruses increase. For smaller values of β , the concentration of cccDNA increases inside the nucleus due the recycling of capsids. Therefore, the number of released virions into the extracellular space increases gradually over time. In a word, recycling of capsids acts as a positive feedback loop in viral replication. In this case, the results indicate that rather than the rapid release of HBV viruses from the infected cell, the accumulation of HBV DNA-containing capsids inside infected cells can play a major role in the exacerbation of infection. A low value of β makes things worse for the sufferer, thus making it difficult to cure. Small virion release rates (β) in the HBV replication process may be a risk factor for chronic hepatitis exacerbation over time. So, this discussion underlines the importance of recycling of capsids in cases of HBV infection.

In Table 3, all the above outcomes that occurred as a result of parameter variation are listed.

Recycling Effect (γ)	Effect of parameter	Uninfected Hepatocytes (X)	Infected Hepatocytes (Y)	HBV DNA-containing Capsids (D)	Hepatitis B Viruses (V)
Not Considered	α increases	Decrease	Increase	Decrease	Increase
Considered	α increases	Increase	Decrease	Decrease	Decrease
Considered	γ increases	Decrease	Increase	Increase	Increase
Not Considered	β increases	Decrease	Increase	Decrease	Increase
Considered	β increases	Increase	Decrease	Decrease	Decrease

Table 3: All the above outcomes occurred as a result of parameter variation.

Remark 2. From the above discussion, it is observed that the role of volume fraction of capsids (α) and virus production rate (β) in infection dynamics are similar in nature.

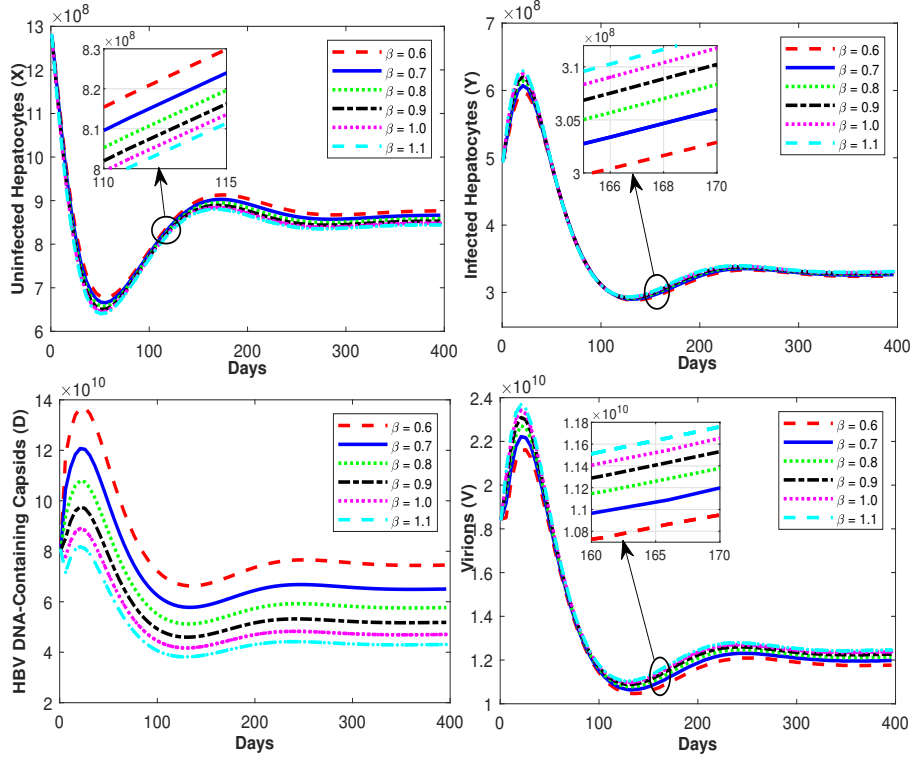


Figure 9: The effects of β in the absence of recycling of capsids ($\gamma = 0$) on the dynamical system (1) w.r.t the initial condition ic_3 .

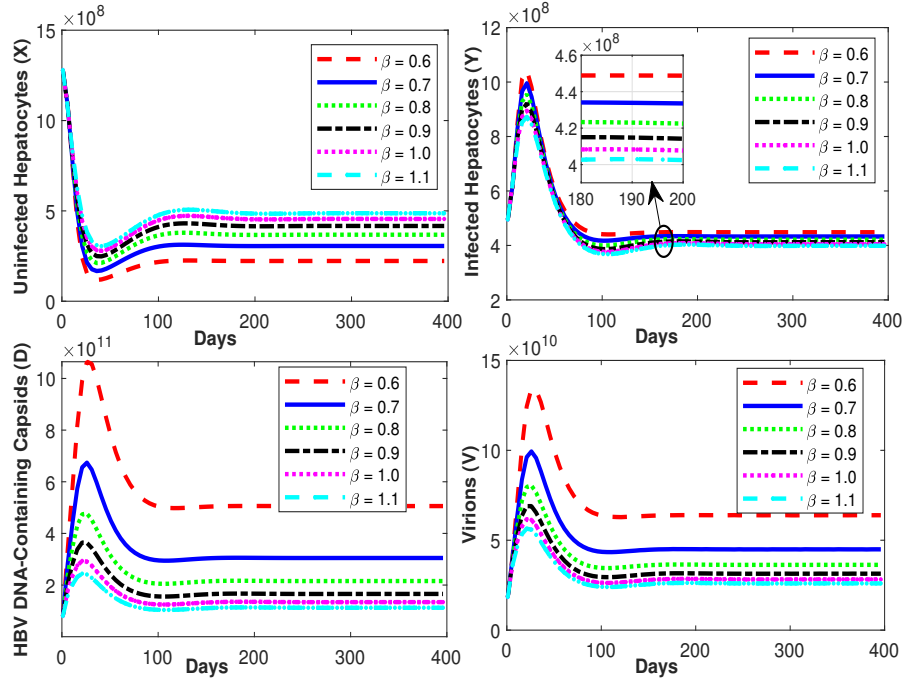


Figure 10: The effects of β on the dynamical system (1) when effects of recycling of capsids is considered ($\gamma > 0$) w.r.t the initial condition ic_3 .

7.4 Elasticities of basic reproduction number with respect to the parameter α , γ and β

The static quantity R_0 depends on the all parameters of the model (1). In the prediction of evolution of HBV, R_0 plays an important role. The sensitivity analysis of R_0 is performed here in order to determine how R_0 responds to changes in parameters. The elasticity of quantity \mathbb{Q} with respect to the parameter

p is denoted by $\mathcal{E}_p^{\mathbb{Q}}$ [39] and given by

$$\mathcal{E}_p^{\mathbb{Q}} = \frac{p}{\mathbb{Q}} \frac{\partial \mathbb{Q}}{\partial p} = \frac{\partial \ln \mathbb{Q}}{\partial \ln p}.$$

In general, elasticity of \mathbb{Q} is positive if it increases with respect to p , and negative if it decreases with respect to p .

$$\begin{aligned} \text{Elasticity of } R_0 \text{ w.r.t } \alpha \quad (\mathcal{E}_\alpha^{R_0}) &= \frac{\alpha}{R_0} \frac{\partial R_0}{\partial \alpha} = \frac{\delta - \gamma}{\alpha(\beta + \gamma) - \gamma + \delta}, \\ \text{Elasticity of } R_0 \text{ w.r.t } \gamma \quad (\mathcal{E}_\gamma^{R_0}) &= \frac{\gamma}{R_0} \frac{\partial R_0}{\partial \gamma} = \frac{(\alpha - 1)\gamma + \delta}{\alpha(\beta + \gamma) - \gamma + \delta}, \\ \text{Elasticity of } R_0 \text{ w.r.t } \beta \quad (\mathcal{E}_\beta^{R_0}) &= \frac{\beta}{R_0} \frac{\partial R_0}{\partial \beta} = -\frac{\gamma(\alpha c \delta - c \delta)}{\alpha \beta c \delta + \alpha c \gamma \delta - c \gamma \delta + c \delta^2}. \end{aligned}$$

One can obtain the followings by using the values of parameters from Table 2:

$$\mathcal{E}_\alpha^{R_0} \approx -1.05, \quad \mathcal{E}_\gamma^{R_0} \approx 0.23 \text{ and } \mathcal{E}_\beta^{R_0} \approx -0.14.$$

This shows that 1% increase in α , β and γ will produce 1.05%, 0.14% decrease and 0.23% increase in R_0 . The sensitivity analysis reveals that α has greater positive impacts on R_0 in magnitude. So, α can be chosen as a disease controlling parameter.

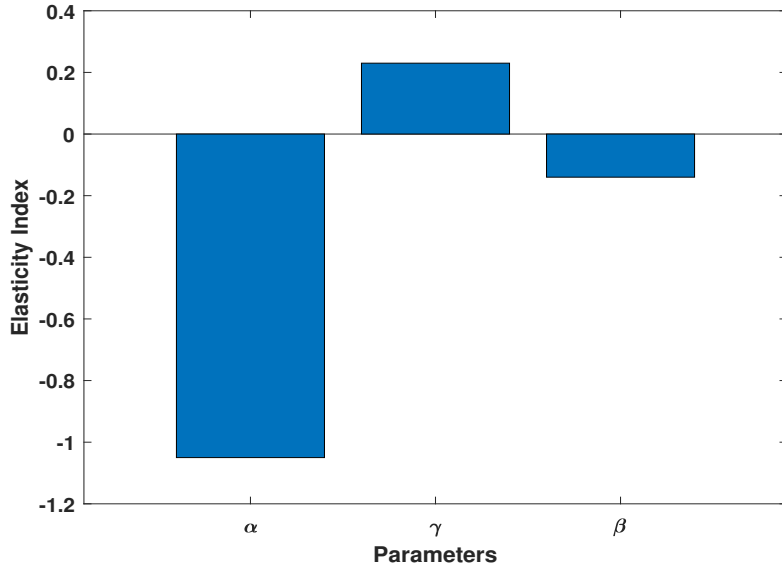


Figure 11: Elasticities of basic reproduction number with respect to parameters α , γ and β .

8 Global sensitivity analysis of the model

The accuracy of results of a mathematical model related to some biological phenomena often becomes poor because of uncertainties in experimental data which are utilized in the estimation of model parameters. Recently, many authors study the effects of single parameter keeping all others parameters fixed at their estimated values. This type of sensitivity analysis is called local sensitivity analysis. But local sensitivity analysis doesn't provide the proper information of uncertainty and sensitivity of the parameters. In order to find out the contributions of each model parameters universally in HBV infection dynamics, the global sensitivity analysis is performed using the technique "Latin hypercube sampling-partial rank correlation coefficient" (LHS-PRCC) described by Marino et al. [43].

8.1 Latin hypercube sampling (LHS)-Partial rank correlation coefficient (PRCC)

Latin hypercube sampling is one kind of Monte Carlo class of sampling methods. In 1979, McKay et al. [45] first introduced this sampling method. With the help of LHS, sample inputs of the model are arranged within a "hypercube of dimensions p ", where p represents the number of model parameters. For our proposed model (1), the number of model parameters (p) is equal to 9. A probability density function (pdf) is employed for sampling parameter values based on parameter ranges partitioned into intervals. In this study, the uniform distribution is chosen for all parameters depending on a priori information and existing data. The model is then simulated iteratively over all p -tuples parameter pairs. It is recommended that the sample size N be at least $(p + 1)$, but it is better to take a larger sample size to ensure the desired accuracy of the results. Here, the sample size is set to 1000.

The correlation coefficient (CC) measures the strength of a linear relationship between the inputs and the outputs. The CC is calculated between the input variable (X) and output variable (Y) as follows:

$$r = \frac{\sum(X - \bar{X})(Y - \bar{Y})}{\sqrt{\sum(X - \bar{X})^2 \sum(Y - \bar{Y})^2}},$$

where \bar{X} and \bar{Y} represent the sample means of X and Y respectively and $r \in [-1, 1]$. In case of raw data of X and Y , the coefficient r is known as sample or Pearson correlation coefficient. The CC (r) is called Spearman or rank correlation coefficient if the data are rank-transformed. By using LHS-PRCC, one can derive insightful conclusions about how the model parameters influence on the outputs of a system. There are several publications that describe the PRCC method in detail [43, 44].

8.2 Scatter plots: The monotonic relationship between input and output variables

Besides the improvement and generalization of a dynamical system, it has attracted the attention of many researchers to know how the outputs are affected if the parameters' values vary in a reasonable range. In the practical field of application especially in virus dynamics model, it is very important and essential to study the sensitivity of parameters. In such cases, PRCC values can provide useful information. PRCC also can assist us to identify which set of parameters is the most significant for achieving some specific goals such as control or regulatory mechanisms, reduce viral load, increase immune response, proposing any new therapy and optimization of drug usage. PRCC is also capable of identifying both positive and negative correlations on model outputs. In order to analyze the sensitivity of parameters, the baseline values are taken from Table 2. To comprehensively analyze the system globally, we opted to vary all parameters from 80% to 120% of their base values. Simulation results of the proposed model (1) are visualized by scatter plots on Figure 13 - Figure 14. The scatter plot for the capsids class is not displayed in this analysis since no substantial distinction is observed when comparing it to the scatter plot of viruses. The PRCC values of all parameters are calculated at day 300 with respect to the dependent variables. The positive correlation of a compartment to a model parameter (PRCC value positive) ensures that if the value of this parameter increases individually or simultaneously, the concentration of the compartment increases accordingly. On the other hand, negative correlation (PRCC value negative) tells us the opposite aspects.

Based on the PRCC values, the model parameters are arranged in descending order for the uninfected, infected, and virus classes as follows:

- **Uninfected hepatocyte:** $\lambda, \alpha, c, \beta, \delta, a, k, \gamma, \mu$.
- **Infected hepatocyte:** $k, a, \lambda, \gamma, \beta, \mu, \delta, c, \alpha$.
- **Virus:** $a, k, \lambda, \gamma, \beta, \mu, \delta, \alpha, c$.

Global sensitivity analysis uncovers numerous new and remarkable findings, which are outlined as follows:

- i The parameters λ, k, a are identified as the most positively sensitive parameters for uninfected hepatocytes, infected hepatocytes, and the viruses. On the other hand, the parameters μ, α, c are found to be the most negatively sensitive parameters for the same entities.

- ii In chronic infection, it has been observed that the virus production rate (β) has a relatively less influence on the overall infection. However, the infection rate (k) itself plays a crucial role in driving and sustaining chronic infection.
- iii The recycling rate (γ) is the second most negatively sensitive parameter for uninfected liver cells. Therefore, the recycling of capsids can indeed act as a positive feedback loop in the context of infection.
- iv The volume fraction of capsids is identified as the most negatively sensitive parameter for the infected compartment. That means if less number of capsids involved in producing new virions and a larger number of capsids undergo in recycling and as a result this would make the infection more severe.

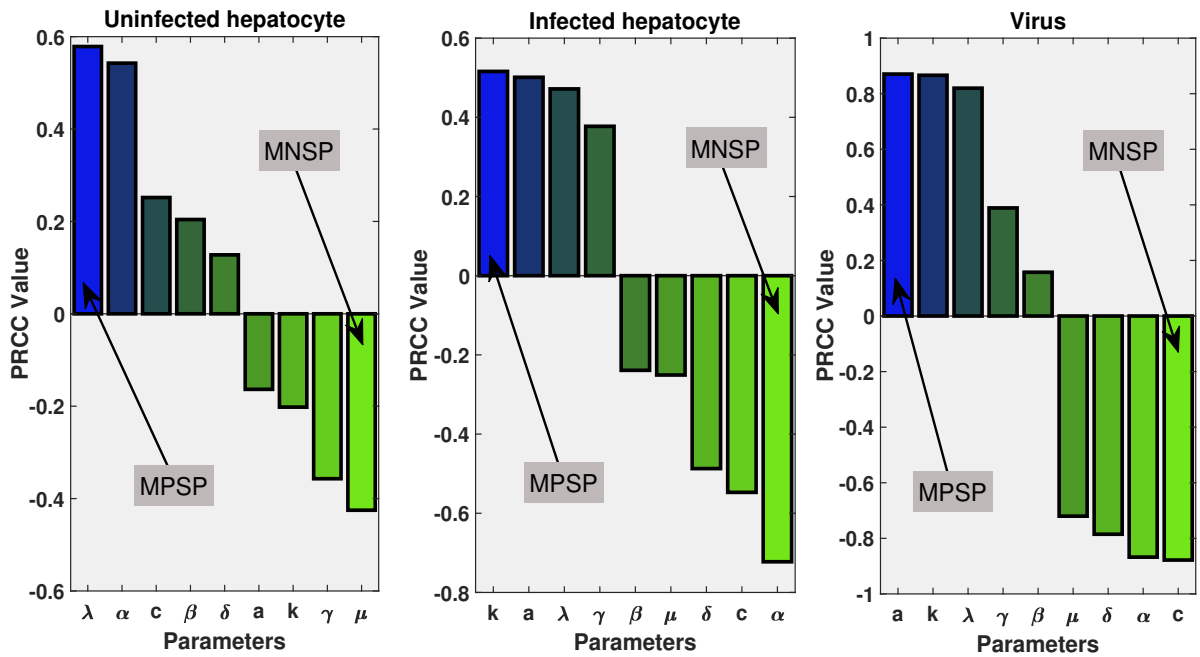
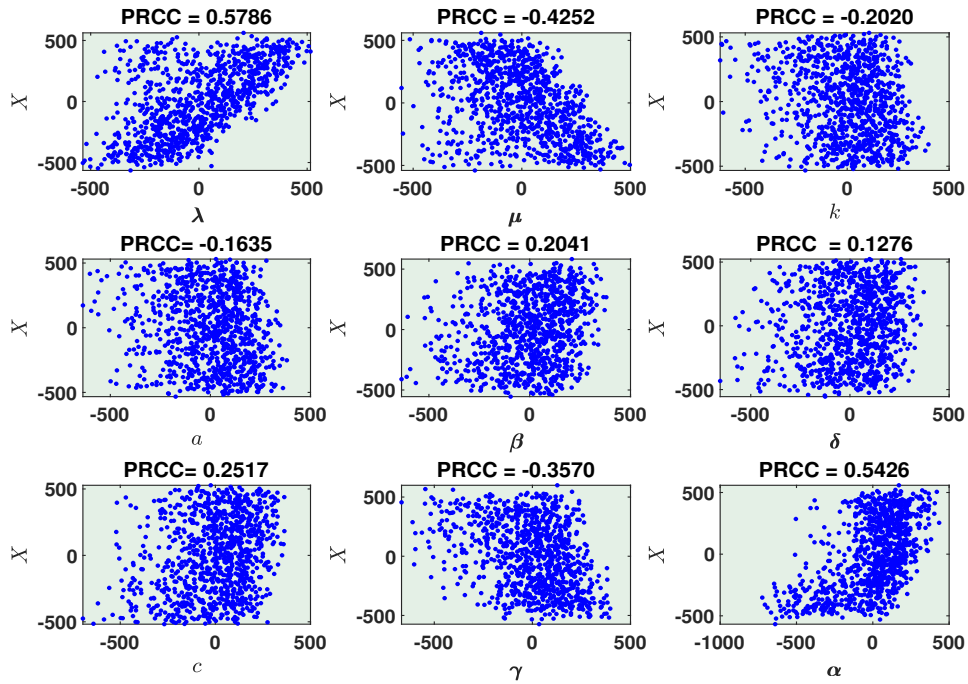
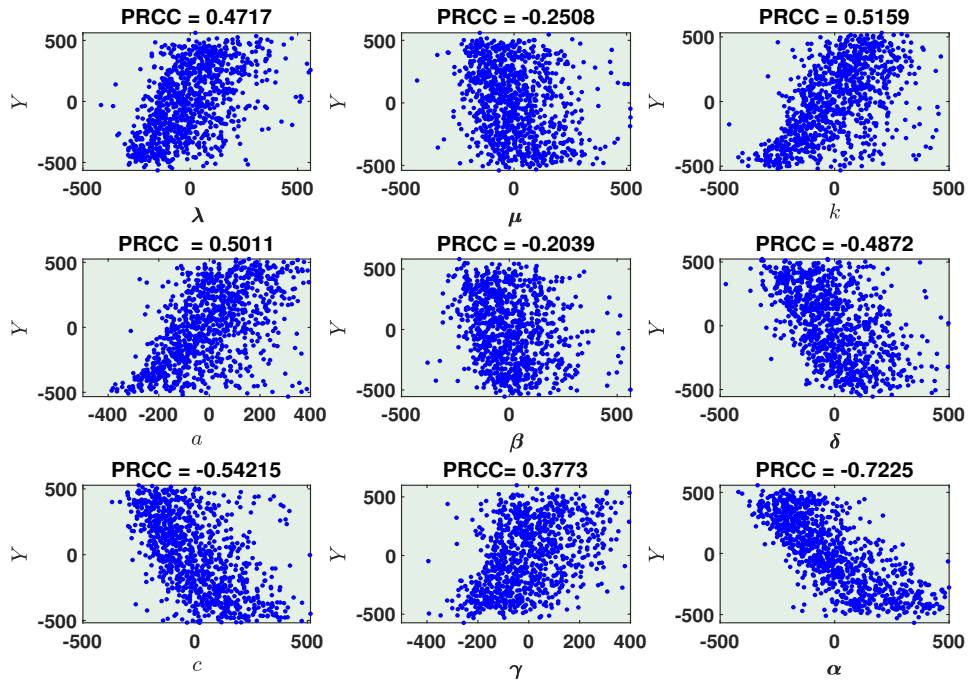


Figure 12: PRCC values of parameters corresponding to uninfected, infected hepatocyte and virus classes are plotted. Here, MNSP: Most Negatively Sensitive Parameter; MPSP: Most Positively Sensitive Parameter.



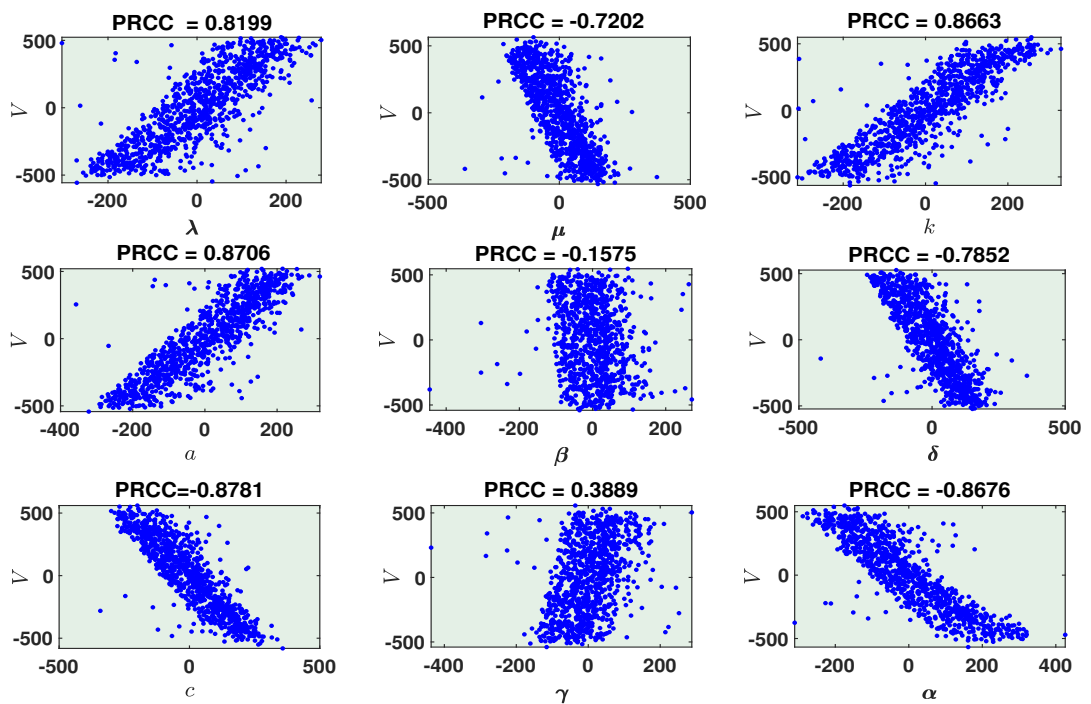
;

Figure 13: Scatter plot for uninfected hepatocytes (X). PRCC value of each parameter are shown on the title on each subplot.



;

Figure 14: Scatter plot for infected hepatocytes (Y). PRCC value of each parameter are shown on the title on each subplot.



;

Figure 15: Scatter plot for Virus (V). PRCC value of each parameter are shown on the title on each subplot.

9 Conclusions

In this present study, hepatitis B virus infection dynamics is modeled based on the biological findings. In order to describe this viral infection in a more realistic way, the recycling effects of capsids are incorporated in this model. By including the recycling effects, we have noticed a paradigm shift in the outcomes of the proposed model. The non-negativity and boundedness of the solutions establish the feasibility of the system. The stability analysis of the system indicates that both the equilibrium points of the proposed model are globally asymptotically stable under some conditions *i.e.* the patient will either achieve a full recovery, or the infection will persist for the rest of the life. Upon comparing the model solution with experimental data collected from four chimpanzees, it is seen that the model solution agrees well with the experimental data. Hence, the proposed model effectively captures and represents the intricate dynamics of HBV infection, making it a more realistic and reliable tool for studying this disease. Comparing with some other relevant studies in the literature, it is also concluded that this model describes richer dynamics behavior of the infection. In addition, it is further observed that due to recycling the viral load increases considerably.

From the simulated results, the following findings are observed.

- (i) Most of the mathematical models on HBV infection developed so far, underestimate the production of virions and suppress the production of capsids as the recycling effects of capsids are ignored. Consequently, these models fail to capture the actual dynamics of HBV infection, whereas, the proposed model shows a more realistic production of virions and the actual dynamics of the infection.
- (ii) Recycling rate of capsids (γ) is one of the deciding parameters in the model to determine the severity of infection. So, it is very important to pay attention to this kind of parameter while proposing any control strategy for this disease.
- (iii) Probably, this study analyses the effects of volume fraction of capsids (α) on disease dynamics for the first time. It is found that the inclusion of recycling of capsids reverses the effects of volume fraction on the infection. This is a striking outcome of the present study that changes the usual understandings about viral dynamics. So, volume fraction of capsids emerges as a viable candidate for a disease-controlling parameter.
- (iv) It is also observed that the number of released viruses increases in spite of low virus production rate due to recycling of capsids. Though this result appears to be contradictory to the known fact, but our study has clearly explained this new findings. In order to gain deeper insights about this infection, the emergence of this unusual behavior becomes very important. On the other word, the recycling of capsids acts as a positive feedback loop in this viral infection.
- (v) Based on the values of Partial rank correlation coefficients, the global sensitivity analysis unequivocally identifies that the disease progression is highly influenced by the volume fraction of capsids as well as recycling rate. These findings highlight the pivotal role of these factors in shaping the dynamics of the disease and warrant further attention in future studies.
- (vi) The strong concurrence between the model solution and the experimental data substantiates that the proposed model is more realistic and reliable.

As mentioned above, our model provides a theoretical backbone of the mechanism causing the exacerbation during the chronic HBV infection. This is a new, and relatively simple mathematical model that can describe the infection dynamics more accurately. Using these new findings, this model can be applied to a variety of clinical trials and for the formulation of new drugs.

Declarations

Ethics approval and consent to participate

Not applicable.

Consent for publication

Not applicable.

Availability of data and materials

Available once the manuscript accepted.

Competing interests

The authors declare that they have no competing interests.

Funding

Council of Scientific & Industrial Research-SRF Fellowship scheme (File No: 09/731(0171)/2019-EMR-I).

Acknowledgments

The first author also thanks the research facilities received from the Department of Mathematics, Indian Institute of Technology Guwahati, India.

Authors' information

Rupchand Sutradhar, Department of Mathematics, Indian Institute of Technology Guwahati, Guwahati, Assam 781039, India. Email: rsutradhar@iitg.ac.in

D C Dalal, Department of Mathematics, Indian Institute of Technology Guwahati, Guwahati, Assam 781039, India. Email: durga@iitg.ac.in

References

- [1] Hepatitis B, <https://www.who.int/news-room/fact-sheets/detail/hepatitis-b>, 24 June 2022 .
- [2] S.A. Whalley, J.M. Murray, D. Brown, G.J. Webster, V.C. Emery, G.M. Dusheiko and A.S. Perelson, Kinetics of acute hepatitis B virus infection in humans. *J Exp Med* 193(7) (2001) 847–854.
- [3] S.M. Ciupe, R.M. Ribeiro, P.W. Nelson, G. Dusheiko and A.S. Perelson, The role of cells refractory to productive infection in acute hepatitis B viral dynamics. *Proc Natl Acad Sci USA* 104(12) (2007) 5050–5055.
- [4] R.M. Ribeiro, A. Lo and A.S. Perelson, Dynamics of hepatitis B virus infection, *Microbes Infect* 4(8) (2002) 829–835.
- [5] S. Lewin, T. Walters and S. Locarnini, Hepatitis B treatment: rational combination chemotherapy based on viral kinetic and animal model studies. *Antiviral Res* 55(3) (2002) 381–396.
- [6] H. Guo, D. Jiang, T. Zhou, A. Cuconati, T.M. Block and J.T. Guo, Characterization of the intracellular deproteinized relaxed circular DNA of hepatitis B virus: an intermediate of covalently closed circular DNA formation. *J Gen Virol* 81(22) (2007) 12472–12484.
- [7] F. Fatehi, R.J. Bingham, E.C. Dykeman, N. Patel, P.G. Stockley and R. Twarock, An intracellular model of hepatitis B viral infection: An in silico platform for comparing therapeutic strategies. *Viruses* 13(1) (2021) 11.
- [8] J.M. Murray, S.F. Wieland, R.H. Purcell and F.V. Chisari, Dynamics of hepatitis B virus clearance in chimpanzees. *Proc Natl Acad Sci USA* 102(49) (2005) 17780–17785.
- [9] C. Saraceni and J. Birk, A review of hepatitis B virus and hepatitis C virus immunopathogenesis. *J Clin Transl Hepatol* 9(3) (2021) 409–418.

- [10] G.M. Prifti, D. Moianos, E. Giannakopoulou, V. Pardali, J.E. Tavis and G. Zoidis, Recent advances in hepatitis B treatment. *Pharmaceuticals* 14(5) (2021) 417.
- [11] Nayeem J, Podde CN and Salek MA, SENSITIVITY ANALYSIS AND IMPACT OF AN IMPERFECT VACCINE OF TWO STRAINS OF HEPATITIS B VIRUS INFECTION, *Journal of Biological Systems*, pp 1-22.
- [12] Ji Y, Min L, Ye Y, Global analysis of a viral infection model with application to HBV infection. *Journal of Biological Systems*, 18(02), pp.325-337, 2010.
- [13] Hui H, Nie LF, Analysis of a stochastic HBV infection model with nonlinear incidence rate. *Journal of Biological Systems*, 27(03), pp.399-421, 2019.
- [14] L. Wang and R. Xui, Mathematical analysis of an improved hepatitis B virus model, *Int. J. Biomath.* 5(1) (2012) 1250006.
- [15] Tchinda PM, Tewa JJ, Mewoli B, Bowong S, A theoretical assessment of the effects of distributed delay on the transmission dynamics of Hepatitis B. *Journal of Biological Systems*, 23(03), pp.423-455, 2015
- [16] Moualeu DP, Mbang J, Ndoundam R, Bowong S, Modeling and analysis of HIV and hepatitis C co-infections. *Journal of Biological Systems*, 19(04), pp.683-723, 2011.
- [17] M.A. Nowak, S. Bonhoeffer, A.M. Hill, R. Boehme, H.C. Thomas, H. McDade, Viral dynamics in hepatitis B virus infection. *Proc Natl Acad Sci USA* 93(9) (1996) 4398–4402.
- [18] D. Wodarz, Hepatitis C virus dynamics and pathology: the role of CTL and antibody responses. *J Gen Virol* 84(7) (2003) 1743–1750.
- [19] K. Wang, A. Fan and A. Torres, Global properties of an improved hepatitis B virus model. *Nonlinear Anal Real World Appl* 11(4) (2010) 3131–3138.
- [20] S. Eikenberry, S. Hews, J.D. Nagy and Y. Kuang, The dynamics of a delay model of HBV infection with logistic hepatocyte growth. *Math Biosci Eng* 6 (2009) 1–17.
- [21] L. Min, Y. Su and Y. Kuang, Mathematical analysis of a basic virus infection model with application to HBV infection. *Rocky Mt J Math* 38(5) (2008) 1573–1585.
- [22] X. Chen, L. Min, Y. Zheng, Y. Kuang and Y. Ye, Dynamics of acute hepatitis B virus infection in chimpanzees. *Math Comput Simul* 96 (2014) 157–170.
- [23] S.A. Gourley, Y. Kuang and J.D. Nagy, Dynamics of a delay differential equation model of hepatitis B virus infection. *J Biol Dyn* 2(2) (2008) 140–153.
- [24] S. Hews, S. Eikenberry, J.D. Nagy and Y. Kuang, Rich dynamics of a hepatitis B viral infection model with logistic hepatocyte growth. *J Math Biol* 60(4) (2010) 573–590.
- [25] G. Huang, W. Ma and Y. Takeuchi, Global properties for virus dynamics model with beddington-deangelis functional response. *Appl Math Lett* 22(11) (2009) 1690–1693.
- [26] Y. Ji, L. Min, Y. Zheng and Y. Su, A viral infection model with periodic immune response and nonlinear CTL response. *Math Comput Simul* 80(12) (2010) 2309–2316.
- [27] F.F. Chenar, Y. Kyrychko and K. Blyuss, Mathematical model of immune response to hepatitis B. *J Theor Biol* 447 (2018) 98–110.
- [28] J.M. Murray, R.H. Purcell and S.F. Wieland, The half-life of hepatitis B virions. *Hepatology* 44(5) (2006) 1117–1121.
- [29] Asabe, Shinichi and Wieland, Stefan F and Chattopadhyay, Pratip K and Roederer, Mario and Engle, Ronald E and Purcell, Robert H and Chisari, Francis V, The size of the viral inoculum contributes to the outcome of hepatitis B virus infection. *Journal of virology* 83(19)(2009) 9652–9662.

- [30] K. Manna and S.P. Chakrabarty, Chronic hepatitis B infection and HBV DNA-containing capsids: Modeling and analysis. *Commun Nonlinear Sci Numer Simul* 22(1-3) (2015) 383–395.
- [31] J. Danane, A. Meskaf and K. Allali, Optimal control of a delayed hepatitis B viral infection model with HBV DNA-containing capsids and CTL immune response. *Optim Control Appl Methods* 39(3) (2018) 1262–1272.
- [32] T. Guo, H. Liu, C. Xu and F. Yan, Global stability of a diffusive and delayed HBV infection model with HBV DNA-containing capsids and general incidence rate. *Discrete Contin Dyn Syst-B* 23(10) (2018) 4223.
- [33] S. Liu and R. Zhang, On an age-structured hepatitis B virus infection model with HBV DNA-containing capsids. *Bull Malaysian Math Sci Soc* 44(3) (2021) 1345–1370.
- [34] J. D. Dias, N. Sarica and C. Neuveut, Early steps of hepatitis B life cycle: From capsid nuclear import to cccDNA formation. *Viruses* 13(5) (2021) 757.
- [35] J. Danane and K. Allali, Mathematical analysis and treatment for a delayed hepatitis B viral infection model with the adaptive immune response and DNA-containing capsids. *High-throughput* 7(4) (2018) 35.
- [36] O. Diekmann, J.A.P Heesterbeek, J.A. Metz, On the definition and the computation of the basic reproduction ratio R_0 in models for infectious diseases in heterogeneous populations. *J Math Biol* 28(4) (1990) 365–382.
- [37] P. Van den Driessche and J. Watmough, Reproduction numbers and sub-threshold endemic equilibria for compartmental models of disease transmission. *Math Biosci* 180(1-2) (2002) 29–48.
- [38] J.M. Heffernan, R.J. Smith and L.M. Wahl, Perspectives on the basic reproductive ratio. *J R Soc Interface*. 2(4) (2005) 281–293.
- [39] M. Martcheva, *An Introduction to Mathematical Epidemiology*, Vol. 61, Springer, (2015).
- [40] L. Perko, *Differential Equations and Dynamical Systems*, Vol. 7, Springer Science & Business Media, (2013).
- [41] T. Kajiwara, T. Sasaki and Y. Takeuchi, Construction of lyapunov functionals for delay differential equations in virology and epidemiology. *Nonlinear Anal Real World Appl* 13(4) (2012) 1802–1826.
- [42] H. Dahari, A. Lo, R.M. Ribeiro and A.S. Perelson, Modeling hepatitis C virus dynamics: Liver regeneration and critical drug efficacy. *J Theor Biol* 247(2) (2007) 371–380. .
- [43] Simeone Marino, Ian B Hogue, Christian J Ray, and Denise E Kirschner. A methodology for performing global uncertainty and sensitivity analysis in systems biology. *Journal of theoretical biology*, 254(1) (2008) 178–196.
- [44] Md Afsar Ali, S.A. Means, Harvey Ho, Jane Heffernan, Global sensitivity analysis of a single-cell HBV model for viral dynamics in the liver. *Infectious Disease Modelling*, 6, (2021) 1220-1235.
- [45] R. J. Beckman McKay, M. D. and W. J. Conover. A comparison of three methods for selecting values of input variables in the analysis of output from a computer code. *Technometrics*, 21(2) (1979) 239–245.

Appendix A Proof of Non-negativity of the solutions

Proof. It is clear that $[\frac{dX}{dt}]_{X(t)=0} = \lambda$, $[\frac{dY}{dt}]_{Y(t)=0} = kVX$, $[\frac{dD}{dt}]_{D(t)=0} = aY$, $[\frac{dV}{dt}]_{V(t)=0} = \alpha\beta D$. Since, $[\frac{dX}{dt}]_{X(t)=0} > 0$, so $X(t)$ is always non-negative $\forall t > 0$.

In order to prove the non-negativity of $Y(t)$, it is essential to show first the non-negativity of $V(t)$. With that aim, it is assumed that $V(t)$ does not satisfy the non-negativity condition *i.e.* \exists a time, say t_V such that,

$$t_V = \inf \left\{ t : t > 0, V(t) = 0, \frac{dV}{dt} \leq 0 \right\}.$$

This implies that $\left[\frac{dV}{dt} \right]_{V(t_V)=0} = \alpha\beta D(t_V) \leq 0$ *i.e.* \exists a time t_D such that

$$t_D = \inf \left\{ t : t > 0, D(t) = 0, \frac{dD}{dt} \leq 0 \right\},$$

which gives $\left[\frac{dD}{dt} \right]_{D(t_D)=0} = aY(t_D) \leq 0$. One may also find a time t_Y such that

$$t_Y = \inf \left\{ t : t > 0, Y(t) = 0, \frac{dY}{dt} \leq 0 \right\}.$$

Clearly, $t_V > t_D > t_Y$. It is clear that $\left[\frac{dY}{dt} \right]_{Y(t_Y)=0} = kV(t_Y)X(t_Y) \leq 0 \implies V(t_Y) \leq 0$. Since, $V(t_Y) > 0$, we arrive at a contradiction to the definition of t_Y . So, $V(t) \geq 0, \forall t > 0$. Consequently, $D(t) \geq 0$ and $Y(t) \geq 0, \forall t > 0$. \square